Accepted manuscript doi:
10.1680/jgeot.18.p.235

Submitted: 18 September 2018

Published online in 'accepted manuscript' format: 17 September 2019

Manuscript title: A Field Investigation into the Mechanisms of Pile Ageing in Sand

Authors: Kenneth Gavin* and David Igoe†

Affiliations: *Faculty of Civil Engineering and Geosciences, Delft University of Technology, Delft, Netherlands and †Department of Civil, Structural and Environmental Engineering, Trinity College Dublin, Dublin 2, Ireland

Corresponding author: David Igoe, Department of Civil, Structural and Environmental Engineering, Trinity College Dublin, Dublin 2, Ireland. Tel.: +353 1 896 3805.

E-mail: igoed@tcd.ie

Accepted manuscript doi:
10.1680/jgeot.18.p.235

Abstract

The design of axially loaded piles has been an area of focus for the offshore industry in recent years. A number of studies report substantial increases in the shaft capacity of piles driven in sand, known as pile ageing. The offshore industry has been slow to implement ageing into practice because of uncertainty over the mechanisms controlling ageing and variability on the impact of ageing. This paper presents the results of tests using an instrumented pile with two separate installations considered, one where the pile was load tested four days after installation and the second where the load test was performed after an ageing period of 116 days. Data from the installation, ageing period, load-testing and pile extraction provide further insights into the mechanisms governing the effect of time on the axial capacity of piles in sand.

Accepted manuscript doi:
10.1680/jgeot.18.p.235

Introduction

The shaft resistance of piles driven in sand exhibits time dependent increases, termed ageing. A number of separate case histories have demonstrated strong increases in pile capacity, up to three-fold over the first 100 days following driving. Despite this, pile ageing has not yet been widely incorporated into design practice because of the combined effects of variability in the degree of ageing indicated by various case studies and uncertainties about the primary mechanisms controlling the process. In this paper the results of field tests on an instrumented open-ended steel pile driven in dense sand are reported. The test programme was designed specifically to measure the radial effective stress and load distribution during installation, ageing and load-testing for a recently installed pile and one that was aged for a period of 116 days. After the ageing period the pile was extracted in order to study the effect of physio-chemical reactions during the ageing period.

Background

A number of workers have reported large gains in capacity with time from field tests performed on piles driven in sand. Tavenas and Audy (1972) found that the axial capacity of driven pre-cast concrete piles increased by approximately 70% over a twenty day period after driving. Similar trends were reported by Fellenius et al. (1989), York et al. (1994), Long et al. (1999), Axelsson (2000a, 2000b), Jardine et al. 2006, Anuscic et al., (2018) and others, see Fig. 1. A simple expression to predict the axial capacity at a given time (Q_t) of the form shown in Eqn. 1 is commonly adopted (see Skov and Denver 1988).

$$Q_t = Q_0 + A \log (t/t_0) \qquad \text{Eq. [1]}$$

Where: A is a constant and Q_0 is the capacity at a reference time t_o.

Significant variability in ageing is evident in Figure 1 where for a given pile-type, time and test-site the pile capacity can vary by more than 50%. Bowman and Soga (2005) and Lim and Lehane (2014) suggest that the scatter evident in these database studies arises from one or a

combination of the following reasons; comparing results of dynamic (DLTs) and static load tests (SLTs), variation in the definition of reference time, load history, difficulty in separating shaft and base resistance from instrumented compression SLTs and combining trends from tension and compression static load tests at different ageing periods

Potential mechanisms for pile ageing were suggested by Chow (1997) including; (i) corrosion and physio-chemical reaction, (ii) stress relaxation and (iii) increased constrained dilation and hence radial stresses with time.

Mechanism 1, corrosion and physio-chemical reactions that develop with time lead to roughening of the pile surface and the growth of a crust of particles adhering to the pile shaft, (see Gavin et al. 2013 and Lim & Lehane 2014). Gavin et al. (2015) suggest corrosion is not the primary mechanism as database studies showed that ageing was observed for steel, concrete and timber piles and occurred both above and below the corrosion zone.

Mechanism 2 involves a gradual breakdown of the hoop stresses developed during pile installation. With time, creep-induced stress redistribution would cause increases in stationary radial effective stress during the set-up period. Particle rearrangement as a result of creep was measured in triaxial ageing tests performed by Bowman and Soga (2003 and 2005) and Kuwano and Jardine (2003). Zhang and Wang (2014) used tactile pressure sensors to measure the stress in the soil mass around a model pile during an 80 hour ageing period following installation in a pile testing chamber. They measured significant redistribution of stress, such that the radial stress increased in areas of low initial stress and reduced significantly in areas of high stress. Modest increases of radial effective stress during ageing (equalisation) have been reported in field tests on pre-cast driven concrete piles by Ng et al. (1988) and Axelsson (2000a), see Figure 2. These increases were seen to occur from very low post-installation values with stresses remaining below the pre-installation horizontal effective stress even after

Accepted manuscript doi:
10.1680/jgeot.18.p.235

ageing. More significant increases were measured for jacked piles by Chow (1997) and Lim and Lehane (2015). The latter report data for piles jacked into three sand deposits in Perth, Western Australia. At these sites radial stresses increased by between 35 and 50% over a 1-day ageing period.

Mechanism 3 involves a modification of soil-structure such that sand in the shear zone exhibits increased confined dilation with time. Schmertmann (1991) notes that time effects are particularly strong for sand that has undergone recent disturbance, for example from dynamic compaction or displacement pile installation. The creep-induced particle rearrangement measured by Bowman and Soga (2003) resulted in a complex structure that resulted in increased dilation during shearing of aged samples in the triaxial apparatus. Axelsson (2000b) reported load tests on a 235 mm square concrete pile installed to a depth of 12.8 m at Fittja Straits, Sweden that was subjected to a number of reload compression tests over a 660 day ageing period. During this period the overall pile capacity increased by 60% although the base resistance remained relatively constant. A radial total stress sensor near the pile toe recorded modest increases due to continued dilation of around 25% during a load test performed 8 days after installation. In a test performed 660 days after installation the sensor recorded a 100% increase due to dilation during loading.

Gavin et al. (2013) reported large increases in radial stress during loading of an open-ended pile driven in dense Blessington sand allowed to age for 219 days. They suggested that this was the primary mechanism for significant ageing of the axial tension capacity of piles tested at this site.

In order to reduce uncertainties identified in previous database studies a series of large-scale pile test programmes were initiated at a number of well-characterised geotechnical test sites including Dunkirk, France (Jardine et al. 2006), Blessington, Ireland (Gavin et al., 2013) and

Accepted manuscript doi:
10.1680/jgeot.18.p.235

Larvik, Norway (NGI, 2014). Details of the piles tested at all sites are shown in Table 1. At each site first-time tension load tests were performed at various periods after installation. Significant increases in pile capacity were evident in most tests, for example the piles at Dunkirk exhibited a 220% increase in shaft capacity in tests performed between 9 and 235 days after installation, See Fig. 3a.

To compare load tests at different sites it is necessary to determine a reference capacity. To avoid ambiguities with regard to assigning a reference time capacity, such as t_0, Gavin et al. (2015), Lehane et al. (2017) and others suggest use of a Cone Penetration Test, CPT based pile design method to perform the normalisation. The pile capacities measured at Dunkirk, Larvik and Blessington are compared in Table 1 with pile capacities estimated using the IC-05 design method (Jardine et al. 2005). It is apparent that the data from the three sites are reasonably consistent and well described by the Intact Ageing Curve, IAC, proposed by Jardine et al. (2006) to describe ageing trends at Dunkirk. However, some scatter remains even in these relatively well controlled tests, with a notable case being the low 30 days pile capacity measured at Blessington.

Significant advances in the design of closed-ended piles in sand were achieved through carefully controlled, instrumented pile tests that measured the radial effective stress on a pile during installation, equalisation and load testing (Lehane 1992 and Chow 1997). The work was synthesized in the CPT based design approaches ICP-05 (Jardine et al. 2005) and UWA-05 (Lehane et al. 2005) which have been shown to provide reliable estimates of pile shaft capacity in sand (Schneider et al. 2007). In order to understand the mechanism of ageing, similar data are required particularly for open-ended piles typically used offshore. This paper presents the results from instrumented pile tests that examined the effect of time since

installation on the radial and shear stress developed on an open-ended pile, driven in dense sand.

Description of Field Tests

Pile tests performed on an instrumented open-ended steel pipe pile are described in this paper. The test pile had an external diameter, D of 340mm diameter and wall thickness of 14 mm. The pile was driven to a tip level 7 m below ground level, bgl and load tested after a set-up period of 116 days (Pile S6). Subsequently it was extracted and re-driven at a new location to a penetration depth of 6.5 m. This pile, designated S7 was and load tested 4 days after installation. The site conditions and test pile details are described in this section.

Site Description

The test site is an active quarry located near the village of Blessington in Ireland. The site has been used to investigate the field response of a number of foundation systems see Gavin et al. (2009), Igoe et al. (2011) and others. The soil at the location is a glacially deposited, dense fine sand with a CPT end resistance, q_c (see Fig. 4a) reported in Igoe and Gavin (2019) that increases from ≈10 MPa near the ground surface to 15 - 20 MPa over the depth of penetration of the test piles. The data in Figure 4a show the average (in bold), maximum and minimum values of CPT q_c measured from eight profiles taken in the vicinity of the test piles. The CPT shaft friction, f_s values in Figure 4b show slightly larger variability with an average friction ratio (f_s/q_c) of 1%.

The water table is approximately 13m below ground level with the result that the sand in which the test pile was embedded is partially saturated. The moisture content of the deposit increases from 8% at ground surface to approximately 12% at 4.5 m depth. The in-situ suction measured used piezometers pushed into pre-drilled auger holes indicate values of between 5 to 10 kPa which are negligible when compared to horizontal effective stresses developed by test piles in this deposit. Laboratory testing was used to supplement the in-situ

site investigation and establish basic soil properties. Particle size analyses classified the material as fine grained, with a median particle size varying from 0.1 - 0.15 mm. Dilatometer testing (DMT) performed at 250 mm depth intervals indicated lift-off and limit pressures that increased rapidly with depth with lift-off pressure in the range of 500-1000 kPa and limit pressures in the range of 2000-3000 kPa over the penetration depth of the test pile, (Figure 5a). Profiles of the estimated coefficient of earth pressure at rest, K_0, based on correlations with the CPT and DMT tests are in good agreement and are shown in figure 5b. Detailed description of the geotechnical properties of Blessington Sand are given in Tolooiyan and Gavin (2013) and Igoe and Gavin (2019).

Pile Instrumentation

The test pile was instrumented with 12 miniature total stress sensors, 20 strain gauges and 10 temperature sensors. The layout of the instrumentation is shown in Figure 6. Three miniature total stress sensors, type TML PDA-PA, were installed at each of four levels (1.5, 5.5, 10.5 and 17.5 diameters from the pile toe). Mechanical protection for the sensor lead wires was provided by two channels which were welded onto the pile outer wall. Each channel was fabricated from two 16 x 16 mm steel strips which formed the channel walls, covered over with a 40 x 3 mm steel strip. The channels were placed diametrically opposite each other and ran the length of the pile, stopping 500 mm from the top of the pile to allow the cables to exit. The strain gauges and temperature sensors were housed inside the channels while the miniature total stress sensors were housed outside the channels and circumferentially offset by ~90 degrees to minimize disturbance caused by the change in geometry due to the channels.

The total stress sensors were placed in pre-drilled slots with the cable exiting through a recessed channel in the pile wall (backfilled with epoxy resin for mechanical protection) which ran into the main steel channels. At the top of the pile the lead-wires were soldered to a

Accepted manuscript doi:
10.1680/jgeot.18.p.235

shielded multi-core cable which was clamped in place. All solders were made using heat shrink solder sleeves to ensure an adequate insulation and protection from moisture ingress. During handling and installation some of the sensors were damaged and unusable for the duration of testing. The decision to provide three miniature total stress sensors at each level (designated A, B and C, See Table 1) was based on experience from installing a previous instrumented test pile at the site (See Gavin et al 2013) where sensor damage during installation occurred. During the first installation, test S6, three sensors were damaged (one near the pile toe, sensor B) and two near the pile head (sensors A and B). During reinstallation of the pile (S7) an additional three sensors were damaged (at h/D levels of 5.5 and 10). Because of the importance of measuring stress near the pile toe, the installation of the pile was stopped at a depth of 6.5 m bgl to prevent further instrument damage and to ensure at least two operational sensors remained at the most important locations. Another limitation of these sensors that should be considered is the potential for shielding of stresses in the sand mass if material adheres to the pile shaft. All strain gauges and temperature sensors remained fully operational throughout the test programme.

Test Results

This section describes the pile performance during the installation, equalization and load test phases.

Pile Installation

The blow-counts required to drive the piles are shown in Figure 7a. Both piles S6 and S7 were driven using a PM20 Junttan piling rig with a 5 tonne HHK-5A hammer. For pile S6, a stroke length of 0.2 m was used for the first 4 m of installation; this was gradually increased to 0.35 m over the last 3 m of driving until the final penetration depth of 7 m was reached. For pile S7 the hammer stroke was varied from 0.2 to 0.5 m. The maximum energy (EMX) transferred into pile S7 was measured during pile driving using accelerometers and strain

Accepted manuscript doi:
10.1680/jgeot.18.p.235

gauges attached to the pile along with a pile driving analyser (PDA). The EMX transferred into pile S6 was estimated based on the hammer properties and drop height. Flynn and McCabe (2016), used EMX measurements with the same piling hammer from multiple sites to determine the Ratio of EMX to rated hammer energy as a function of drop height, showing a strong linear correlation. Using a best-fit linear trend line through the data, the following equation was used to estimate the EMX for pile S6:

$$\boldsymbol{EMX} = \left(\frac{100 - \Delta \boldsymbol{E}_{\boldsymbol{cushion}}}{100}\right) \times \left(-0.06 + 112.86.\boldsymbol{h}_{\boldsymbol{avg}}\right) \times \boldsymbol{E}_{\boldsymbol{rated}} \qquad \text{Eq. [2]}$$

Where $\Delta \boldsymbol{E}_{\boldsymbol{cushion}}$ is the percentage energy loss due to the piling cushion (assumed to be 20%) and h_{avg} is the average hammer drop height and E_{rated} is the rated energy of the hammer (59 kNm). A comparison of the energy from both piles is provided in Figure 7c and explains the significantly higher blow counts from S6 compared with S7. Despite the different blow counts noted during installation, both piles provide a very good match with the ageing pile capacity trend from identical piles installed at the site (S2 – S5, Gavin et al. 2013) indicating that the end of driving capacity was not significantly affected by the blow counts.

Driving was paused at intervals of 0.25 m to record the stationary radial stress and soil plug length. The Incremental Filling Ratio (IFR, is the change in plug length per increment of pile penetration) is shown in Figure 7b for Pile S6. The pile was almost fully coring (IFR > 85%) for the first 2m of penetration. Below this depth IFR reduces with depth with a final IFR value at 7m of 40%. Unfortunately, the plumb line used to measure the IFR profile for pile S7 was damaged at the start of installation and therefore it was not possible to record the IFR for pile S7.

The stationary radial stresses measured in pause periods during the installation of pile S6 are shown in Figure 8. Since the sand is partially saturated and previous model pile tests indicated no pore pressure build up during installation, the stationary radial stresses are

assumed to be equivalent to the short-term radial effective stresses (σ'_{rs}). It is evident that for a given sensor depth a relatively wide variation of σ'_{rs} was measured, for example the sensor at h/D = 1.5 recorded σ'_{rs} values in the range 188 to 560 kPa at depths between 3 m and 6 m. Part of this variability may be due to instrument zero shifts, the small sensing face, soil smear or they could reflect geological variability. For these reasons it is difficult to verify the absolute values of the sensor readings (laboratory calibration of these sensors is extremely difficult because of the complex boundary conditions involved, see Kirwan, 2015 and Zhu et al. 2009). Nonetheless, the general response of the sensors was consistent for both the tests described in this paper and in agreement with the trends noted in Gavin et al. (2013). During pile installation to 3 m bgl, the radial stress values at all h/D levels, were scattered around the estimated in-situ horizontal stress, σ'_{h0}. During driving, when the sensors were located at depths in excess of 3 m, the depth coinciding with onset of plugging (see Figure 7c), the radial stresses increased significantly, being 2 to 6 times higher than σ'_{h0}, with the higher ratios measured at the sensors closest to the pile tip (h/D = 1.5 and 5.5).

The strain gauges allowed the residual load that developed during installation to be estimated. At the end of installation of Pile S6, a significant residual load existed, See Figure 9. The peak load measured near the pile tip was 364 kN, which corresponds to a base pressure of ≈ 4.2 MPa or ≈ 20% of the q_c value at the pile tip. Gavin and Lehane (2007) report base residual stresses of between 2.4 MPa and 7.3 MPa developed by a jacked, open-ended pile at the test site, with the residual stress increasing as IFR reduced. Interestingly for pile S6 the residual load at all levels on the pile dropped in the 40 minute monitoring period following the end of driving, with the value near the pile tip reducing by 40%, see Figure 9. Given that elastic decompression of the pile would occur almost instantaneously following the last

hammer blow, the reduction of the residual load in this period must have been associated with relaxation in the soil mass.

Ageing Period

Following installation a battery powered Campbell Scientific cr800 data-logger was used to provide measurements of the radial stress every 30 mins for the duration of the ageing period on the test piles. The values measured on both piles were comparable and data from the Pile S6 with the longer ageing period are shown in Figure 10. The following trends are noteworthy;

1. Immediately after installation the radial stresses were highest near the pile tip (h/D = 1.5 and 5.5).
2. The radial stress at all h/D levels reduced over time, with the largest reductions occurring nearest the pile tip (at h/D=1.5 and 5.5). Notable reductions in radial stresses occurred in the hours immediately following pile driving, with reductions of 10 to 15% of the peak values measured at h/D = 1.5 and 5.5 over the first 24 hours.
3. These reductions in radial stresses continued over the entire ageing period though they appeared to be reaching asymptotic values (at least for sensors remote from the pile base) after ~100 days. This tendency for radial stress to reduce with time is in agreement with previous measurements from pile S5 at the same site (Gavin et al. 2013). However it contrasts with the data shown in Fig. 2 which increased with time, however, at all sites there is a tendency for the measured stress to approach the in-situ horizontal stress before pile installation suggesting recovery of installation damage as hypothesized by Lim and Lehane (2014).

The data are recast in Figure 11 in which profiles of the radial effective stress profile with depth at various times (0 to 100 days) during the ageing period are compared to the σ'_{rc} profiles predicted using the IC-05 and UWA-05 CPT methods for open-ended piles. Also

Accepted manuscript doi:
10.1680/jgeot.18.p.235

shown in Figure 11b are data from Gavin et al., (2013) measured during a 220 day ageing period on Pile S5. It is evident, that whilst the design methods under-estimate the installation stress, given they are calibrated to predict the medium-term (10-30 day) stress they provide reasonable estimates for the appropriate time period. It is evident that for the sensors remote from the pile tip (h/D = 10.5 and 17.5), the horizontal stress measured at the pile-soil interface reduces to long term values which are very close to the estimated in-situ σ'_{h0}. For the two sensor levels nearest the pile tip, the effect of plugging during installation (below 3 m) and the presence of large residual loads in the vicinity of the pile base, result in radial stresses which remain significantly higher than σ'_{h0}.

It is clear that the effects of installation, particularly the plugging effect led to large increases in vertical and horizontal stresses around the test piles. For the dense Blessington sand, these stresses were considerably higher than the pre-installation in-situ stress and following installation, much lower far-field σ'_{h0} and σ'_{v0} values existed. From the strain gauges data (residual load) and radial stress sensors, it appears that stress redistribution lead to reductions in radial stress near the pile shaft and vertical stress at the pile base.

Load Testing

The load displacement response of piles S6 and S7 during maintained load static tension tests performed 116 days 4 days after driving respectively are shown in Figure 12. The tests were performed using a fully automated load controlled hydraulic system. The test procedure involved 40 kN load steps, with the load maintained for 5 mins at each increment. The data are compared to load tests performed on the same site on identical 7 m long piles S2 to S5 reported by Gavin et al. 2013 (data shown by dotted lines) and reveal;

The pile capacity increased significantly with time from 340 kN one day after installation to approximately 1,000 kN after 116 days. The one-day tension capacity is comparable to the

Accepted manuscript doi:
10.1680/jgeot.18.p.235

residual load developed at the end of installation, see Figure 9. The capacity of piles tested 116 and 219 days after installation were very similar suggesting the pile developed its maximum resistance during the first five months. As Pile S7 had a slight smaller penetration length to allow direct comparison the average shaft resistance (q_{sav}) developed during pile loading is plotted in Figure 12b. This shows that q_{sav} increased from 45 kPa to a peak of 140 kPa due to the ageing period, however, the initial pile stiffness up to q_{sav} of 25 kPa did not vary with time.

For the two pile tested in the current series, during testing of Pile S6 large creep displacements were noted when the load exceed 1020 kN at a displacement of ≈ 3.5% of the pile diameter (≈ 12 mm). For pile S7 significant creep occurred at a pile head load of 400 kN and the pile reached failure as defined by a displacement of 10% of the pile diameter during this loading step with the load increasing as the pile moved downward.

Measurements of the radial stresses during the load tests are shown in Figure 13. The radial stress response of Pile S6 is broadly comparable to measurements from the aged pile S5 reported by Gavin et al. (2013). The following points are noted:

- For pile S6 that was allowed to age for 116 days, Figure 13 all sensors show slight reductions in the radial stress at the start of the load test. The sensors closest to the pile tip (h/D = 1.5 and 5.5) then measured significant increases in radial stress ~240kPa and ~150 kPa at h/D=1.5 and 5.5 respectively as the pile displacement increased. The small reduction at the start of loading is most likely due to the change in loading direction from compression during installation to tension in the load-test, See Lehane (1992) and Chow (1997).
- At the upper sensor levels, (h/D=10.5 and 17.5) stress reductions occurred throughout the load-test.

- For pile S7, load tested 4 days after installation, the radial stresses at the bottom of the pile (h/D=1.5) increased initially by ~20 – 30 kPa, before reducing to lower than pre-test values at higher load levels.
- At all other sensor levels on pile S7, the radial stresses reduce initially before increasing at the higher load levels, however, at the peak-load the values are similar to pre-test values.

The strain gauges placed at multiple levels along the shaft of pile S6 and S7 allowed the distribution of load and shear stresses along the pile to be determined, See Figure 14. The self-weight of the internal soil plug was estimated to contribute less than 1% (<10kN) to the tension capacity and was thus ignored in the shear stress calculation. It is apparent from the data, see figure 4 that the load transfer and shear stress mobilized between ground level and 3 m bgl. was relatively low. The majority of the resistance developed by both piles was in the region from 3 m to 7 m bgl, with shear stresses being much higher near the pile tip. During the ageing period the shear stress in the region between 3 m and 7 m bgl. increased significantly whilst those closer to ground level did not appear to change. For comparative purposes the radial stress measured at the peak load were converted to shear stresses (assuming Mohr-Coulomb behaviour with an interface friction angle of 29º) are shown as squares on Figure 14b. The back-calculated values are in good agreement with the measured data providing confidence in the reliability of the radial stress measurements and suggesting that the shear resistance is fully mobilised during the load test.

Pile Extraction and Observation

After the load tests were completed the sand around the pile was carefully excavated around and the pile was removed from the ground. In keeping with observations from Chow et al. 1988, Lehane et al. 2012 and others a cemented crust of sand was found to be adhered to the side of the aged piles, S5 (Gavin et al., 2013) and S6 over the lower 4 to 5 m of the pile shaft,

See Figure 15a. Yang et al. (2010) describe three distinct layers that formed on their model piles and a similar structure developed on Pile S6. The first layer, See Figure 15b was cemented to the pile shaft and was very difficult to remove. The second and third layers were attached to the first layer and remained adhered to the pile when extracted from the ground, but could be removed with moderate effort. The second and third layers were comparable to zones 1 and 2 described by Yang et al. (2010), while the first layer was deemed to have been originally a zone 1 material which had become bonded to the steel shaft through physiochemical processes.

Energy-Dispersive X-ray Spectrometry (EDS) was conducted on samples taken from the different layers and soil samples taken recovered from a sonic coring borehole located adjacent to the areas in which the piles were installed. The purpose was to investigate if any changes in the chemical composition of the sand occurred during the ageing period. The EDS spectra from all samples revealed predominantly quartz with some calcite and occasional hints of kaolinite. In the borehole samples very little calcium was seen in the sample spectra. However, calcium was detected in in nearly all the samples recovered from the pile. Some spectra from the cemented layer showed almost equal amounts quartz and calcium with large amounts of iron present also, indicating that chemical bonding occurred with the steel pile. The authors suggest the increased calcium in samples taken from the pile shaft could relate to chemical bonding between the sand and calcium bicarbonates precipitating out of the pore water, as suggested by Kirwan (2015). Whilst the number of EDS spectrums from each sample was too small for any meaningful statistical analysis, there was a very marked difference in the spectrums of samples taken from the borehole to those from the pile shaft.

Accepted manuscript doi:
10.1680/jgeot.18.p.235

In addition to the EDS analysis, the roundness and sphericity of the samples taken from the pile shaft and borehole samples were determined using Scanning Electron Microscopy (SEM) and J-image software for image processing. The roundness, R, was determined as follows:

$$R = \frac{4A_c}{\pi L_{major}^{\ 2}} \qquad \text{Eq. [3]}$$

Where A_c is the cross sectional area of the particle and L_{major} is the length of the major axis. The sphericity, S, was determined as the ratio of the largest inscribed circle to the radius of the circumscribed circle centred at the particles centre of mass. From the borehole samples taken, very little variation was noted with depth with average roundness values of 0.595 and sphericity values of 0.503. For samples taken from the layer 1 and 2 material from the pile shaft, a slight increase (of approximately 10%) in roundness and sphericity was noted with average values of 0.638 and 0.556 respectively. Such slight differences would not be significant enough to cause any notable difference in the mechanical behaviour of the sand. These findings are generally in agreement with the laboratory measurements of zone 1 and 2 material described by Yang et al. (2010).

The presence of an adhered crust of sand on the aged piles would lead to migration of the shear failure plane from the pile-soil interface to the sand mass. The increase in the operational friction angle from 29º (pile-soil), see Doherty et al. (2012) to the constant volume friction angle of ϕ'_{cv} = 36º would lead to an increase in mobilised shear stress of approximately 30%. It is worth noting that it is possible that the growth of the crust could lead to the radial stress sensors on the pile wall being somewhat shielded from the radial stress gradient away from the pile, and may also partly explain the reductions in radial stress measured.

Accepted manuscript doi:
10.1680/jgeot.18.p.235

Conclusions

Radial stress and load distributions measured from two instrumented open-ended driven pile tests drive in dense sand revealed:

1. Large radial stresses were generated during pile installation that were significantly higher than the in-situ horizontal stress. Continuous measurements of the radial stress measured after installation show the radial stresses (particularly near the pile toe) reduce over time but remain above the in-situ horizontal stress. The radial stresses after 30+ days were comparable to predicted radial stresses from recent CPT based design methods. The reduction in radial stress over time with one hypothesis that ageing is caused by breakdown of the circumferential stress can lead to an increase radial stress over time. It is possible however that the growth of a cemented crust on the pile surface may have shielded the sensors from the radial stress gradients away from the pile.
2. During tension static load testing, very large increases in radial stress due to dilation were noted for piles which had been allowed to age for more than 100 days. A static tension test on a comparable pile 4 days after driving shows slight reductions in the radial stresses during loading indicating that increased confined dilation was the primary mechanism for pile ageing at Blessington.
3. After load testing, the aged piles were extracted from the ground and examined. A notable crust was adhered to the pile shaft for piles left in the ground for several months, which could be defined as three distinct layers. EDS spectrums from samples taken from each layer indicated that physiochemical processes, possibly involving ground-water, caused some chemical bonding of the sand particles to the pile shaft.

Accepted manuscript doi:
10.1680/jgeot.18.p.235

Based on findings of these experiments and previous work by other researchers, the authors suggest that tendency for the tension resistance of a pile driven in sand to increase with time is due to a combination of time-dependent processes involving stress redistribution, particle rearrangement and physio-chemical processes.

Acknowledgements

The authors would like to acknowledge the support of Science Foundation Ireland and would also like to thank the following industry partners for their on-going support: Mainstream Renewable Power, Bullivant Taranto and Lloyds Acoustics. The authors would like to further thank the following colleagues and technical staff at University College Dublin who provided invaluable help during the instrumentation of the piles and field tests; Lisa Kirwan, Paul Doherty, Tim Hennessy, Weichao Lee and Frank Dillon.

Nomenclature

A	Ageing factor
A_c	Cross sectional area of particle
bgl	below ground level
CPT	Cone Penetration Test
D	external pile diameter, m
DLT	Dynamic Load Test
EDS	Energy-Dispersive X-ray Spectrometry
EMX	Maximum Driving Energy imparted to pile
E_{rated}	Rated energy of piling hammer
$\Delta E_{cushion}$	percentage energy loss due to the piling cushion
F_s	CPT sleeve friction
h	distance from pile toe, m
h_{avg}	average hammer drop height
IFR	Incremental Filling Ratio, %
IAC	Intact ageing curve
L_{major}	Length of the particle major axis

Accepted manuscript doi:
10.1680/jgeot.18.p.235

K_0	coefficient of earth pressure at rest
Q_t, Q_o	Pile capacity at time t and t_0 respectively
SLT	Static Load Test
PDA	Pile Driving Analyser
P_L	Dilatometer limit pressure
P_O	Dilatometer lift-off pressure
p_{ref}	reference pressure, kPa
q_c	CPT cone resistance, MPa
q_{sav}	Average shaft resistance
R	pile outer radius, m
SEM	Scanning Electron Microscope
t	time
t_o	A reference time
UCD	University College Dublin
UWA	University of Western Australia
δ_f	interface friction angle at failure, degrees
ϕ'_{cv}	Constant volume friction angle
σ'_{rs}	stationary radial effective stress on a pile, kPa
σ'_{ho}	Horizontal effective stress prior to pile installation, kPa
τ_f	shaft friction at failure, kPa

References

Anusic, I. Lehane, B, Eiksund, G.R. Liingaard, M.A. (2018) Evauation of installation effects on the set-up of field displacement piles in sand, Canadian Geotechnical Journal, In Press.

Axelsson (2000a) Long term set-up of driven piles in sand, PhD Thesis, Dept. of Civil and Environmental Engineering. Stockholm: Royal Institute of Technology. Set-Up of Driven Piles in Sand

Axelsson, G. (2000b) Effect of Constrained Dilatancy During Loading, Proceedings of the International Conference on Geotechnical and Geotechnical Engineering, GeoEng 2000, Melbourne, Australia.

Bowman, E.T. and Soga, K (2003) Creep, ageing and microstructural change in dense granular materials, Soils & Foundations, Vol. 43 (4), pp 107-117

Bowman, E.T. and Soga, K (2005) Mechanisms of setup of displacement piles in sand: laboratory creep tests, Canadian Geotechical Journal, Vol. 42, Number 5, October, pp 1391-1407

Chow, F. (1997) 'Investigations into behaviour of displacement piles for offshore structures'. *PhD Thesis,* University of London (Imperial College).Chow, F. C., Jardine, R. J., Brucy, F., and Nauroy, J. F. (1998). "Effects of time on capacity of pipe piles in dense marine sand." J. Geotechnical and Geoenviron. Eng., 124(3), 254–264

Fellenius, B.H., Riker, R.E., O'Brein, A.J. and Tracy, G.R. (1989), Dynamic and static testing in soil exhibiting set-up, Journal of Geotechnical Engineering, ASCE, Vol. 115

Flynn, K., McCabe, B. (2016) Energy transfer ratio for hydraulic pile driving hammers, Civil Engineering Research in Ireland (CERI) conference, Galway, Ireland. doi.org/10.13025/S8V881

Gavin K.G. and O'Kelly B.C. (2007). "Effect of friction fatigue on pile capacity in dense sand", Journal of Geotechnical and Geoenvironmental Engineering, ASCE, Vol. 133, No. 1, pp 63-71.

Gavin K.G. and Lehane B.M.. (2007) Base Load-Displacement Response of Piles in Sand' Canadian Geotechnical Journal, Vol. 44, No. 9, September 2007, pp 1053-1063.

Gavin K.G., Adekunte, A. and O'Kelly, B. (2009) A field investigation of vertical footing response on sand. Proceeding of ICE, Geotechnical Engineering, Vol.162, Issue GE5, pp 257-267, DOI 10.I 680/geng.2009.I 62.5.257, October 2009

Gavin, K., Cadogan, D. Tolooiyan, A and Casey, P. (2013) The base resistance of non-displacement piles in sand. Part I, Proceedings of the ICE – Geotechnical Engineering, Volume 166, Issue 6, April 2013 pages 540 –548

Igoe, D, Gavin, K.G. and O'Kelly, B. (2011) The shaft capacity of pipe piles in sand, ASCE Journal of Geotechnical and Geoenvironmental Engineering,(2011) Vol 137, No.10, pp 903-912 DOI 10.1061/(ASCE)GT.1943.5606.0000511.

Igoe, D. and Gavin, K. (2019) Characterization of the Blessington Sand Geotechnical Test Site, Aims Gesociences, Volume 5, Issue 2, 145–162

Gavin, K. Igoe, D and Kirwan, L. (2013. The effect of ageing on piles in sand, ICE Journal of Geotechnical Engineering Vol. 166, Issue 2. April 2013.

Gavin, K., Jardine, R.J., Karlsrud, K. and Lehane, B.M.(2015). The Effects of Pile Ageing on the Shaft Capacity of Offshore Piles in Sand. Proc. international Symposium Frontiers in Offshore Geotechnics (ISFOG), Oslo. p 25.

Jardine, R. Chow, F. Overy, R. and Standing, J. (2005) 'ICP Design Methods for Driven Piles in Sands and Clays', In: Thomas Telford, Ed. London: University of London (Imperial College). Dunkirk

Jardine, R, Standing, J. and Chow, F. (2006). Some observations of the effects of time on the capacity of piles driven in sand. Geotechnique Vol 55, No. 4, pp 227-244.

Karlsrud, K., Jensen, T.G, Wensaas Lied, E.K, Nowacki, F, and Simonsen, A.S. (2014), Significant ageing effects for axially loaded piles in sand and clay verified by new field load tests. Proceedings of the Offshore Technology Conference, Houston, May 2014, Paper No. OTC-25197-MS.

Kirwan, L. (2015) Investigation of ageing mechanisms for axially loaded piles in sand, PhD thesis, University College Dublin

Kuwano, R. & Jardine, R.J. 2002. On measuring creep behav-iour in granular materials through triaxial testing. Canadian Geotechnical Journal. Vol. 39, No.5, pp 391-395.

Lehane, B. (1992) 'Experimental investigations of pile behaviour using instrumented field piles', *Civil Engineering*. London: University of London (Imperial College). Labenne

Lehane B.M., R.J. Jardine, A.J. Bond and R. Frank (1993), "Mechanisms of shaft friction in sand from instrumented pile tests", ASCE Journal of. Geotechnical. Engineering., ASCE

Lehane, B. Schneider, J. and Xu, X. (2005) 'A review of design methods for offshore driven piles in siliceous sand', *Report no. GEO:05358*. Perth: University of Western Australia

Lehane, B.M. Schneider, J.A, Lim, J.K. and Mortara, G. (2012), Shaft Friction from Instrumented Displacement Piles in an Uncemented Calcareous Sand, Journal of Geotechnical and Geoenvironmental Engineering, Vol. 138, No. 11, November 1, 2012.

Lehane, B.M. Lim, J.K. Carotenuto, P. Nadim, F. Lacasse, S. Jardine, R.J. and van Dijk, B. (2017), Characteristics of Unified Database for Driven Piles, Proceedings of 8th International Conference of Offshore Site Investigation and Geotechnics, Lond

Lim, J.K., and Lehane, B.M. (2014). Characterisation of the effects of time on the shaft friction of displacement piles in sand. Géotechnique, 64(6): 476-485.

Lim, J.K. and Lehane, B.M. (2015). Time effects on the shaft capacity of jacked piles in sand. Canadian Geotechnical J. Vol. 52, No. 11, pp 1830-1838.

Long, J.H., Kerrigan, J.A. Wysockey, M.H. (1999) Measured time effects for axial testing of driven piling, Transport Research Board, 1663, No.1, pp 8-15.

Ng, E., Briaud, J.L and Tucker, L.M. (1988), Field Testing of 5 Axially Loaded Single Piles in Sand at Hunter's Point",Research Report to FHWA, Geo Resource Consultants Inc., San Francisco, California, USA.

Norwegian Geotechnical Institute (2014) Time effects on pile capacity. Summary and evaluation of test results, Report 20061251-00-279, Rev.1 March 2014.

Schmertmann, J.H. (1991) The Mechanical Aging of Soils, ASCE Journal of Geotechnical Engineering, Vol.117, Issue 9, pp 1288-1330

Schneider, J., White, D. and Lehane, B. (2007) Shaft friction of driven piles in siliceous, calcareous and micaceous sands. In Offshore site investigations and geotechnics: Confronting New Challenges and Sharing Knowledge. Society of Underwater Technology. 367 – 382.

Skov, R., and Denver, H. 1988. Time-dependence of bearing capacity of piles. In Proc. 3rd Int. Conf. on the Application of Stress-Wave Theory to Piles. Edited by B.G. Fellenius. Vancouver, BC, Canada: BiTech Publishers, Ottawa, Canada. pp. 879-888.

Tavenas, F,. and Audy, R. (1972), Limitations of the driving formulas for predicting bearing capacities of driven piles in sand, Canadian Geotechnical Journal, Vol. 9, No.1, pp 47-62.

Tolooiyan, A and Gavin, K.G, (2013) The base resistance of non-displacement piles in sand, Part II – Numerical Analyses, ICE Journal of Geotechnical Engineering, Vol 166, 6, pp 549-560.

Yang, Z.X., Jardine, R.J., Zhu B.T., Foray, P. and Tsuha, C.H.C.. 2010. Sand grain crushing and interface shearing during displacement pile installation in sand, Géotechnique, Vol 60, No 6, pp 469-482.

York, D. L., Brusey, W.G., Clemente, F. M., and Law, S. K. (1994). Setup and Relaxation in Glacial Sand, Journal of Geotechnical Engineering, Volume 120, No. 9, ASCE, pp. 1498-1513.

Zhang, Z. and Wang, Y.H. (2014), Examining Setup Mechanisms of Driven Piles in Sand Using Laboratory Model Pile Tests, Journal of Geotechnical and Geoenvironmental

Engineering, ASCE, ISSN 1090-0241/04014114(12), Published online December 2nd, 2014.

Zhu, B., Jardine, R. J. & Foray, P. (2009). "The use of miniature soil stress measuring cells in laboratory applications involving stress reversals", Soils and Foundations, Vol. 49, No. 5, pp 675-688.

Table 1 Ageing pile tests at Dunkirk (*estimates at Blessington based on local CPT profiles)

Site	**Pile Dimensions**	**Pile No.**	**Time (days)**	**Pile Capacity (kN)**	**Pile Capacity normalised by IC-05 prediction***
Dunkirk (Jardine et al. 2006)	457 mm diameter, 18.9-19.3 m long	DK1 DK2 DK3	9 81 235	1445 2420 3221	1.03 1.72 2.29
Karlsrud et al. (2014)	508 mm diameter, 20.1m long	1 2 3 4 5	42 132 213 365 730	980 990 1160 1065 1080	2.37 2.40 2.81 2.58 2.62
Gavin et al. (2013)	340 mm diameter, 7 m long	S2 S3 S4 S5	2 12 30 219	344 665 385 990	0.82 1.55 0.90 2.22

Table 2: Summary of radial stress sensor performance after installation

Instrument	Distance from toe (m)	Level (h/D)	Pile S6			Pile S7		
TML PDA-PA (rated capacity of 3MPa or 500kPa)	0.51	1 (1.5)	A	~~B~~	C	A	~~B~~	C
	1.87	2 (5.5)	A	B	C	~~A~~	B	C
	3.57	3 (10.5)	A	B	C	~~A~~	~~B~~	C
	5.95	4 (17.5)	~~A~~	~~B~~	C	~~A~~	~~B~~	C

Accepted manuscript doi:
10.1680/jgeot.18.p.235

List of Figures

Accepted manuscript doi:
10.1680/jgeot.18.p.235

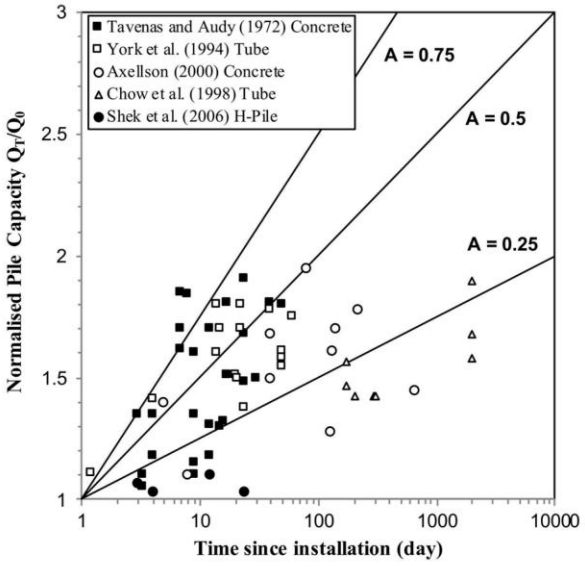

fig1

Accepted manuscript doi:
10.1680/jgeot.18.p.235

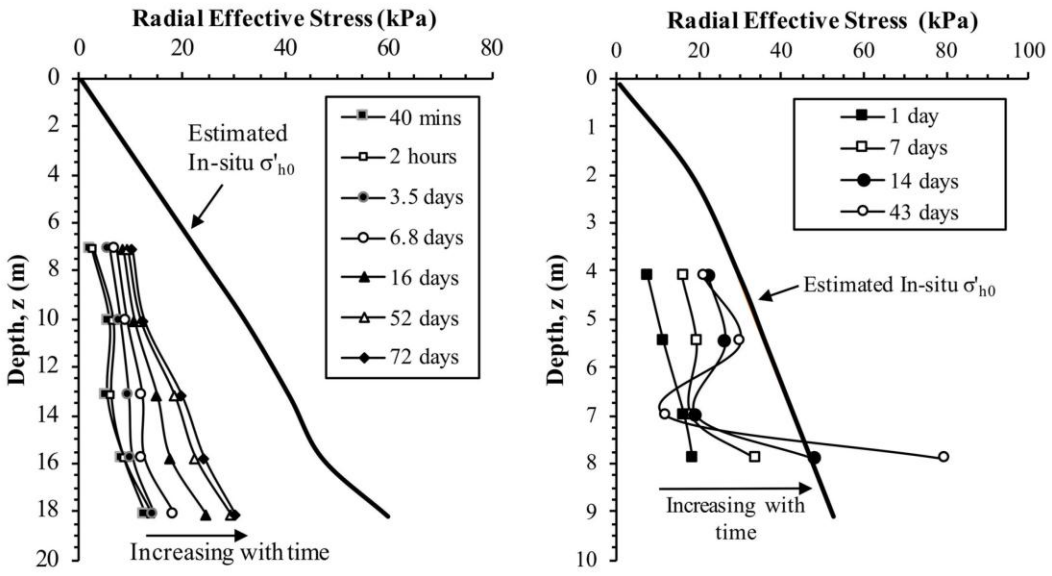

fig2

Accepted manuscript doi:
10.1680/jgeot.18.p.235

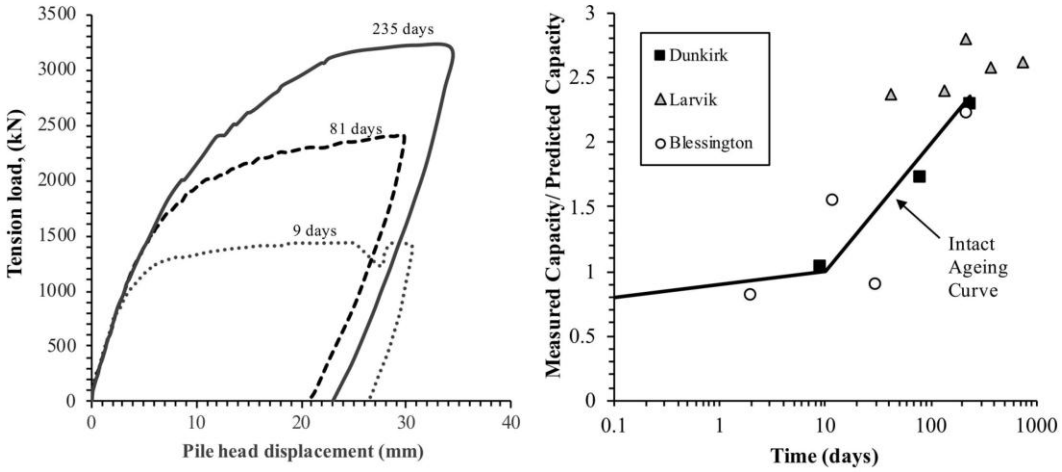

fig3

Accepted manuscript doi:
10.1680/jgeot.18.p.235

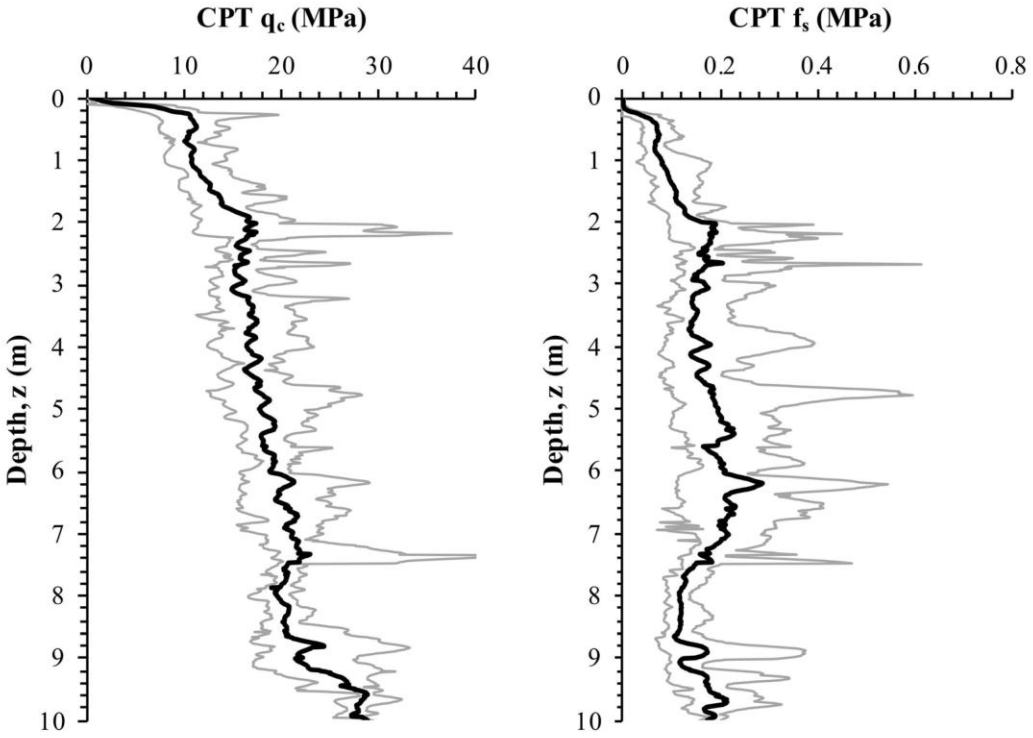

fig4

Accepted manuscript doi:
10.1680/jgeot.18.p.235

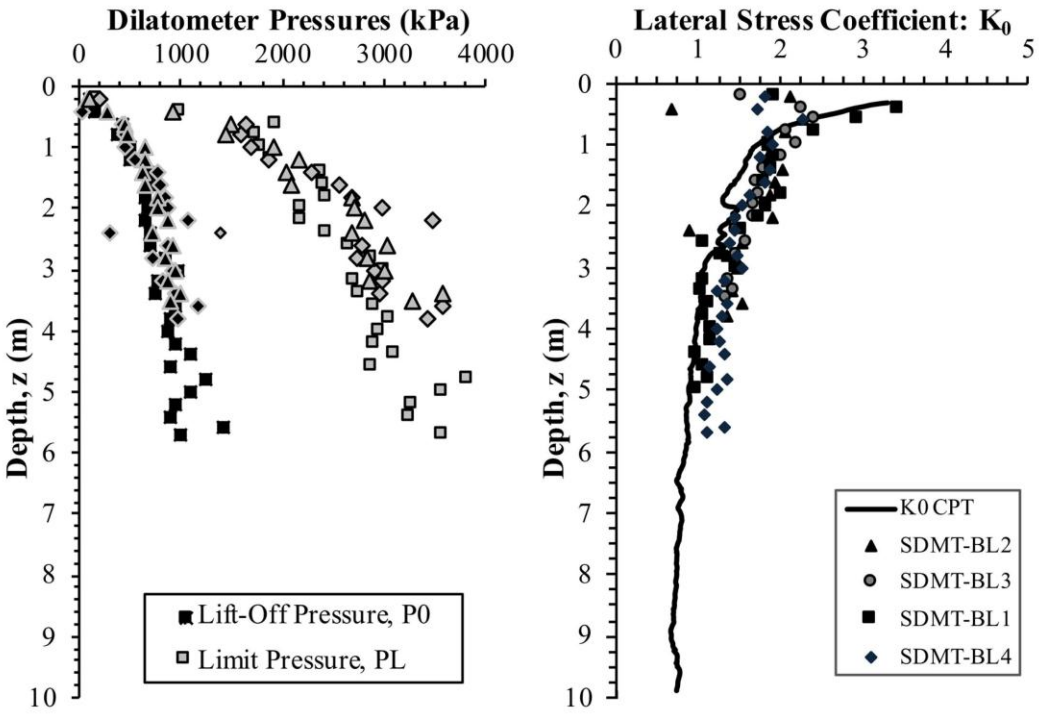

fig5

Accepted manuscript doi:
10.1680/jgeot.18.p.235

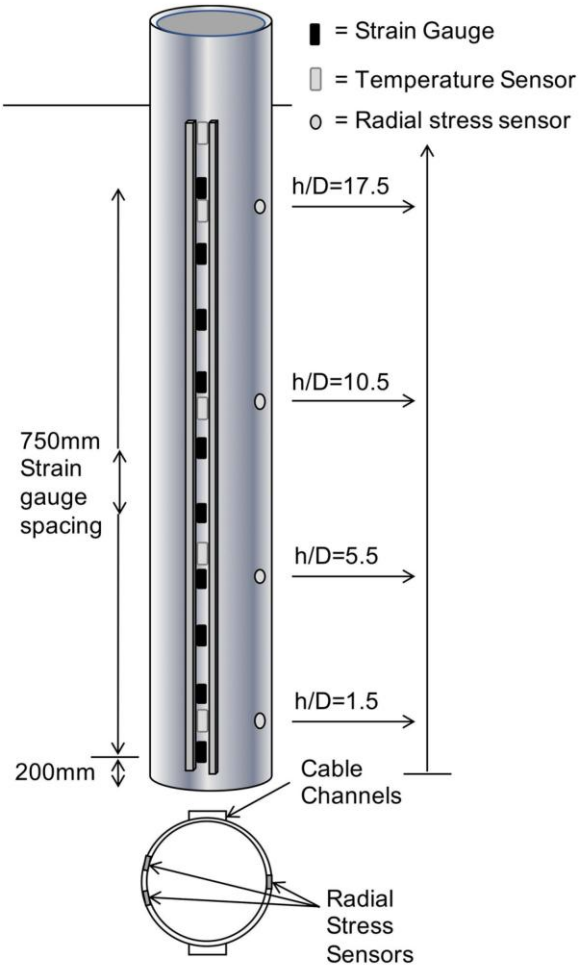

fig6

Accepted manuscript doi:
10.1680/jgeot.18.p.235

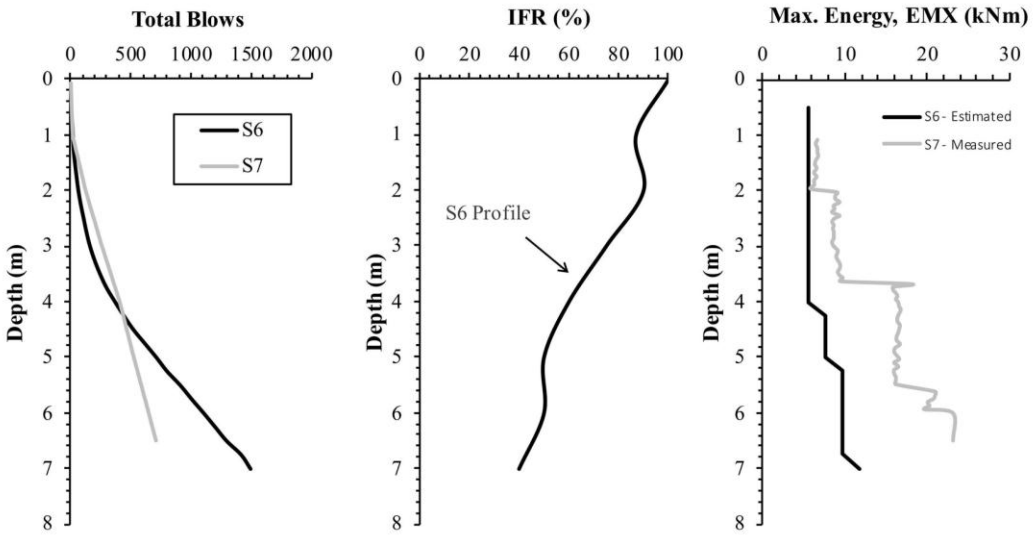

fig7

Accepted manuscript doi:
10.1680/jgeot.18.p.235

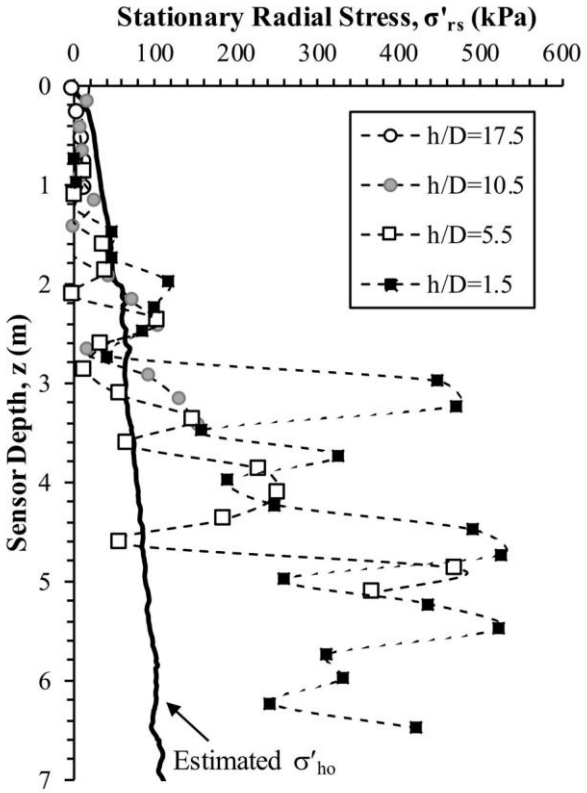

fig8

Accepted manuscript doi:
10.1680/jgeot.18.p.235

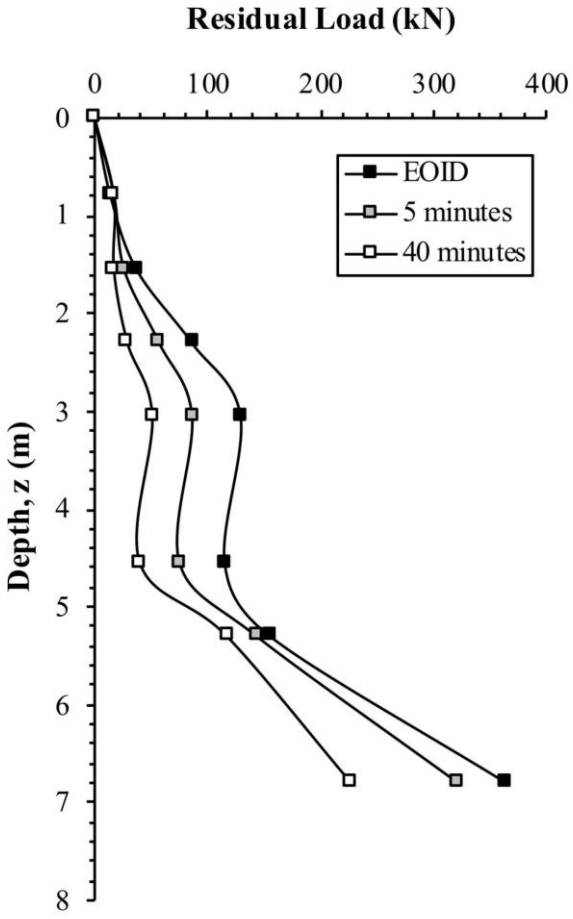

fig9

Accepted manuscript doi:
10.1680/jgeot.18.p.235

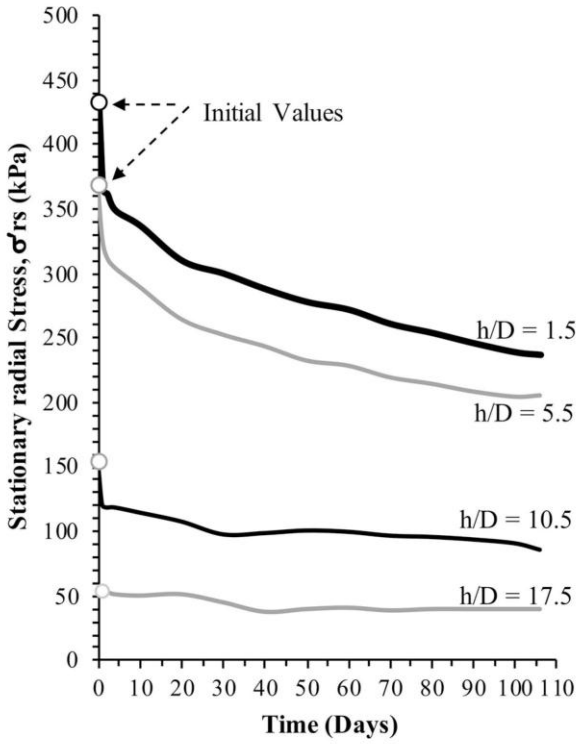

fig10

Accepted manuscript doi:
10.1680/jgeot.18.p.235

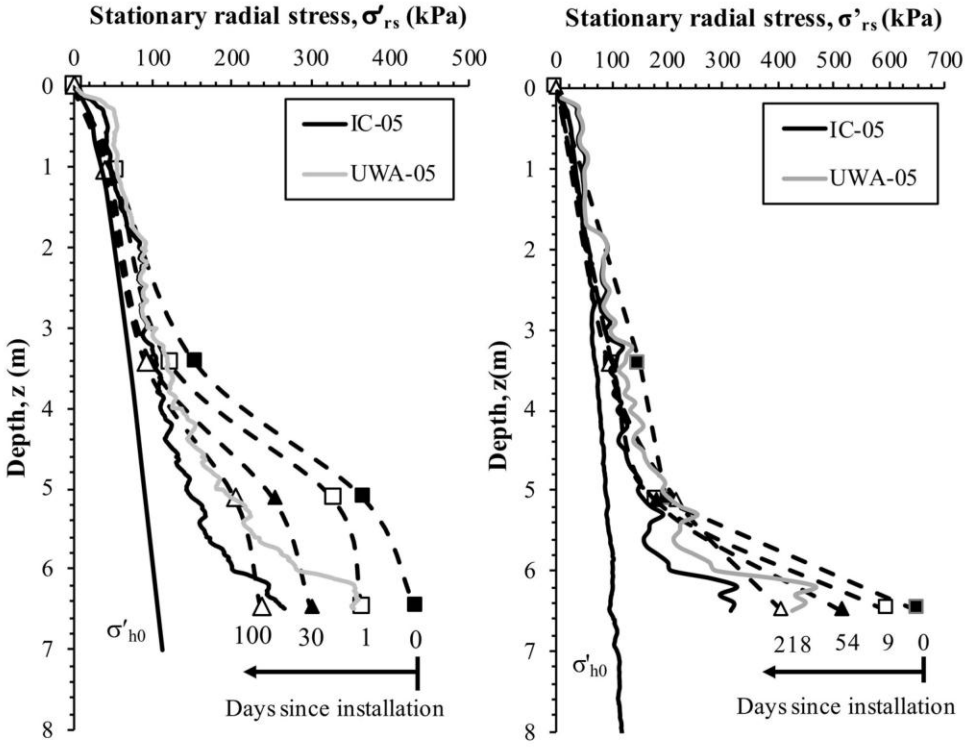

fig11

Accepted manuscript doi:
10.1680/jgeot.18.p.235

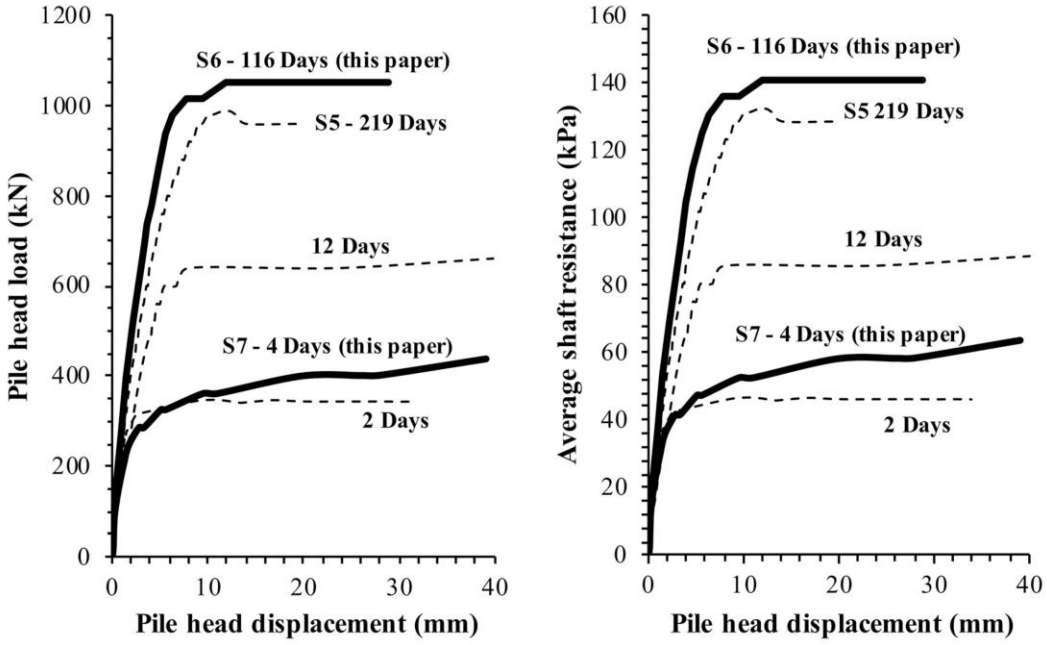

fig12

Accepted manuscript doi:
10.1680/jgeot.18.p.235

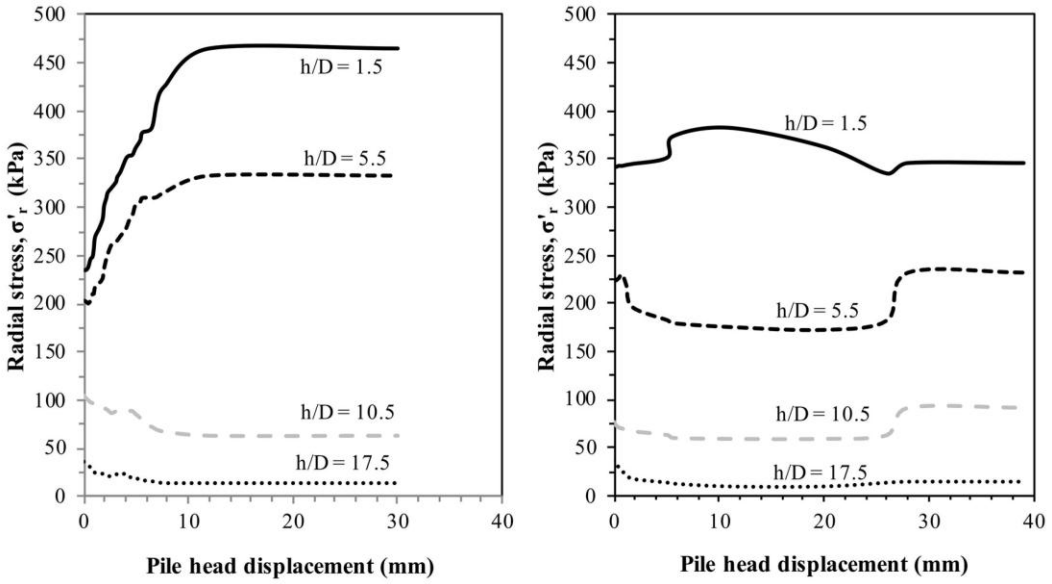

fig13

Accepted manuscript doi:
10.1680/jgeot.18.p.235

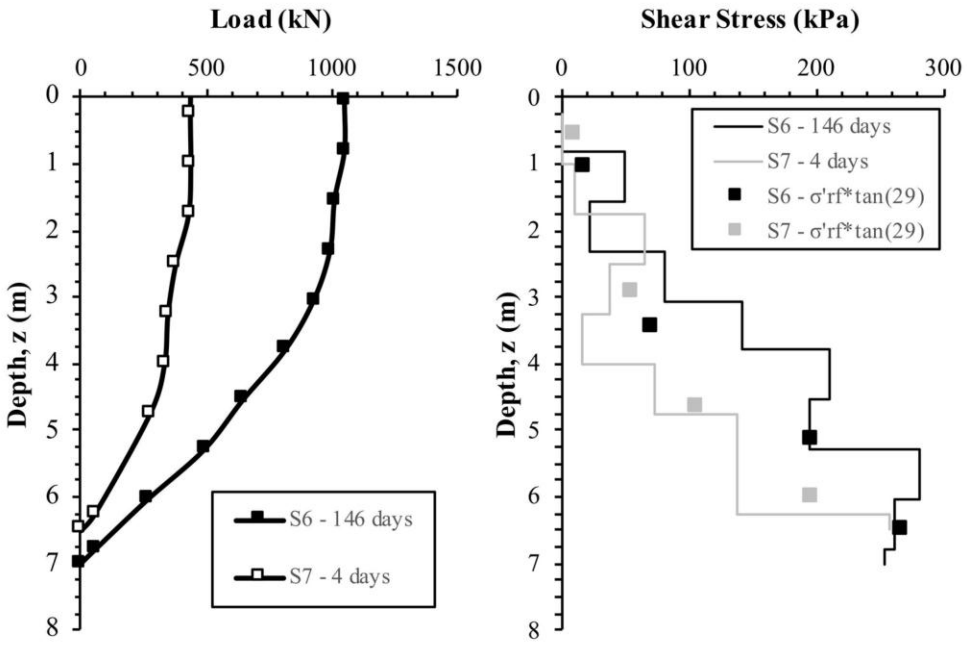

fig14

Accepted manuscript doi:
10.1680/jgeot.18.p.235

fig15